Available online at www.sciencedirect.com
ScienceDirect
ELSEVIER
Nuclear Instruments and Methods in Physics Research A 566 (2006) 465–471
NUCLEAR INSTRUMENTS & METHODS IN PHYSICS RESEARCH Section A
www.elsevier.com/locate/nima

Influence of radioactive filiation on measured release curves

G. Lhersonneau[a,*], A.E. Barzarkh[b], V. Rizzi[a], O. Alyakrinskiy[a], K.A. Mezilev[b], F.V. Moroz[b], V.N. Panteleev[b], L.B. Tecchio[a]

[a]*INFN, Laboratori Nazionali di Legnaro, Viale dell'Università 2, 35020 Legnaro (PD), Italy*
[b]*Petersburg Nuclear Physics Institute, Leningrad district 18850 Gatchina, Russia*

Received 21 June 2006; accepted 15 July 2006
Available online 10 August 2006

Abstract

Perturbation of measured release curves of radioactive nuclei by the decay of precursor nuclei in the target is investigated. The target is described by a simple model taking into account the direct production of the nucleus of interest by the reaction but also allowing decay of the isobaric precursor to take place specifically during diffusion or effusion. Their respective contributions to the observed ion currents can be enough different to lead to uncorrect analysis of the experimental release curves. As an example we discuss release curves of the pairs of neutron-rich isotopes (^{86}Rb^{m}, ^{91}Rb) and (^{130}Cs^{m}, ^{139}Cs) produced by proton-induced fission at the IRIS facility, Gatchina.

PACS: 29.25.Rm; 29.30.Kv

Keywords: Isotope separation on-line; Release time; Decay in target

1. Introduction

The efficiency of on-line mass separation of radioactive nuclei critically depends on how fast the release of these nuclei from the target material is. Since the advent of on-line mass separators devoted to decay spectroscopy in the 1970s, considerable effort has been invested to study release properties, see e.g. a review by Kirchner [1] and other proceedings of EMIS conference series. Recently, these studies have got a new impetus owing to the development of Radioactive-Ion-Beam (RIB) projects based on the isotope separation on-line. In Europe, the next generation of RIB facilities shall be the Italian SPES [2] and French SPIRAL-II [3] whose aim is to provide beams of neutron-rich nuclei in the $A = 80$–150 mass range at energies somewhat exceeding the Coulomb barrier on most targets. The INFN-Legnaro, GANIL, Petersburg Nuclear Physics Institute (PNPI) and IPN-Orsay laboratories have joined efforts to study yields and release properties of various target configurations using the on-line separator located at the IRIS facility, Gatchina. These studies are also carried out in the framework of the planned European radioactive beam facility EURISOL [4]. Neutron-rich nuclei are produced by fission of natural uranium induced by 1 GeV protons. As a consequence of the broad distribution of cross-sections for nuclide production, the more neutron-rich isobars of the nuclei of interest are formed with sizeable amounts. They contribute to its creation via β decay in the target. This causes a delayed production after the accelerator beam pulse. The aim of the present paper is to present a formalism to allow this effect to be quantified and to give guide lines to select nuclei to be used for release time measurements.

2. Experimental frame

For producing neutron-rich nuclei at the future RIB facilities SPES, SPIRAL-II and EURISOL a two-stage method is proposed. Fission shall be induced by secondary neutrons produced by the reactions of a primary charged-particle beam of protons or deuterons. For the sake of measuring release properties, in our experiments at PNPI Gatchina, fission is induced by a beam of 1 GeV protons

*Corresponding author. Tel.: +39 049 8068410; fax: +39 049 641925.
E-mail address: gerard.lhersonneau@lnl.infn.it (G. Lhersonneau).

0168-9002/$ - see front matter © 2006 Elsevier B.V. All rights reserved.
doi:10.1016/j.nima.2006.07.030

impinging on a UC_x target. Reports on recent experiments carried out in this context can be found in Refs. [5–7].

In most release-time measurements γ spectroscopy is used to measure the current of radioactive ions. Sequences of accelerator beam on/off cycles are repeated until sufficient statistics is reached. In our measurements at PNPI the mass-separated ions are collected on a tape for an interval Δt after which the tape is moved (transport time 1.25 s) to a remote counting station. The decay radiation is counted for the same time Δt, during which another sample is collected. If the mother element is not ionised and does not contribute via its decay on the tape the equations are very simple. The number of collected nuclei $n(t)$ is obtained by solving

$$\mathrm{d}n(t)/\mathrm{d}t = i(t) - \lambda n(t) \tag{1}$$

where $i(t)$ is the ion current impinging on the tape and λ is the radioactive constant of the collected nucleus. The equations are solved with $n(t_j) = 0$ at the begin of each jth time bin. The number of nuclei collected before transport is $n_j = n(t_j + \Delta t)$. The number of decays during the counting bin is

$$N_j = \mathrm{e}^{-\lambda t_{\mathrm{tr}}} \lambda \int_0^{\Delta t} n_j \mathrm{e}^{-\lambda t}\, \mathrm{d}t \tag{2}$$

where t_{tr} is the transport time. The set of N_j values forms the experimental release curve. As a matter of fact, if Δt is small with respect to time constants, N_j is closely proportional to the average value of $i(t)$ during the jth collection bin. This way, one obtains a good approximation of the time dependence of the ion current. The method is rather direct but measurements are restricted to nuclei with radioactive lifetimes not much shorter than 1 s due to transport at each counting time bin.

Alternatively, placing a detector facing the collection spot, collection and counting can be simultaneous. The tape is at rest during the accelerator beam-on/off cycle and is moved only before a new irradiation starting a new cycle. Release times measured in that way were recently reported by the IPN-Orsay group [8]. This allows to measure very short-lived nuclei far from stability on the falling slope of cross-sections. The observed activity curve is an integral of the release curve observed with the method at PNPI and thus less directly related to the release function.

In the following, we first consider the finite duration of irradiation on the release curve of a nucleus only produced by the beam. Then we introduce the feeding by mother decay.

3. Model

3.1. General considerations

The release function $R(t)$ to be determined can be regarded as the response of the separator, as an outgoing ion current, to a short pulse of the accelerator at time $t = 0$. In practice, the observable is a *release curve* in which the true release function is folded with the probability to create the nucleus of interest with time, be it during irradiation of the target, which has to be long enough to accumulate counting statistics, or via β decay of its more n-rich parent. The ion current to the tape is given by the following expression:

$$i(t) = \varepsilon\phi(t) \tag{3}$$

$$\phi(t) = \int p(t')R(t - t')\,\mathrm{e}^{-\lambda(t-t')}\,\mathrm{d}t' \tag{4}$$

where $i(t)$ is the ion current, ε is the time independent efficiency including ionisation and transport of the ion beam (occurring with neglectible delay), $\phi(t)$ the flux of atoms reaching the ioniser, $p(t')$ is the in-target production rate at time t', t is the time of observation of the current and λ the radioactive decay constant of the nucleus.

The direct production in fission follows the beam profile:

$$\begin{aligned} p(t') &= p \quad \text{for } t' \in [-t_{\mathrm{ir}}, 0] \\ p(t') &= 0 \quad \text{for } t' > 0 \end{aligned} \tag{5}$$

where t_{ir} is the duration of irradiation and the origin of time $t = 0$ has been set at the end of irradiation.

The contribution from β decay depends on the number of mother nuclei present in the target

$$p_\beta(t') = \lambda_1 n_1(t') \tag{6}$$

where $n_1(t')$ is the number of mother atoms, with radioactive constant λ_1, in the target (in the following we shall use the index 1 for the mother and 2 for the nucleus of interest while the index 2 shall be implicit on the left-hand side of equations with indexed variables). This number obviously grows steadily when the beam is switched on and remains non-zero for some time after the beam has been switched off. This different time behaviour thus disturbs the observed release curve. This effect shall be investigated in a following section.

The release function is a convolution of diffusion and effusion. In Ref. [9] Kirchner quotes formulae giving the flux of atoms per time unit for diffusion for various geometries of the target matter and for effusion in the empty space in between ('void'). A common characteristics of diffusion formulae is that they are expressed as a series of exponentials. Their amplitudes and time constants are correlated and are described by a single parameter μ_0, often associated with a release time via $\mu_0 = \ln(2)/T_{\mu,1/2}$, although this relation only holds for a single component. With little additional complication of the formalism we use a series of exponentials of free amplitudes and time constants,

$$D(t) = \sum a_k \mu_k\, \mathrm{e}^{-\mu_k t} \tag{7}$$

which is normalised by $\sum a_k = 1$. Effusion is simply described by a single exponential function with constant v:

$$E(t) = v\mathrm{e}^{-vt}. \tag{8}$$

Following the assumption quoted by Kirchner that at our target temperature range of 1900–2200 °C an effusing atom shall not reenter the matter, the processes are treated sequentially. Combining diffusion and effusion the value of the release function observed at time t is

$$R(t) = \int_0^t D(t')E(t-t')\,\mathrm{d}t' \tag{9}$$

where $D(t')\,\mathrm{d}t'$ is the number of atoms produced at time $t=0$ completing diffusion in $[t', t'+\mathrm{d}t']$ and $E(t-t')$ is the effusion function for atoms starting to effuse at time t'. After inserting the expressions for diffusion and effusion it reads

$$R(t) = \sum_k \frac{a_k \mu_k \nu}{\nu - \mu_k}(\mathrm{e}^{-\mu_k t} - \mathrm{e}^{-\nu t}). \tag{10}$$

The behaviour of each $R_k(t)$ term is dominated by the smallest (μ_k, ν) constant, i.e. by the longest time constant. A consequence is that a non-zero effusion time shall eventually 'cut' the infinite series of diffusion after a finite number of terms.

The principle of the calculation is displayed in Fig. 1. Solid and dashed lines represent the beam profile (rectangle) and activity of a nucleus (i.e. the creation rate of its daughter), respectively. For each of them an element of flux $\mathrm{d}\phi(t-t')$ produced by nuclei created during a time slice $[t', t+\mathrm{d}t']$ is shown.

This example is calculated with $T_{1/2} = 10$, diffusion in spherical grains with $\mu_0 = \ln(2)/5$ and $\nu = \ln(2)/5$, where times are in arbitrary units. The β decay activity curve and the corresponding flux element (dashed lines) have been multiplied by 10 to be better visible.

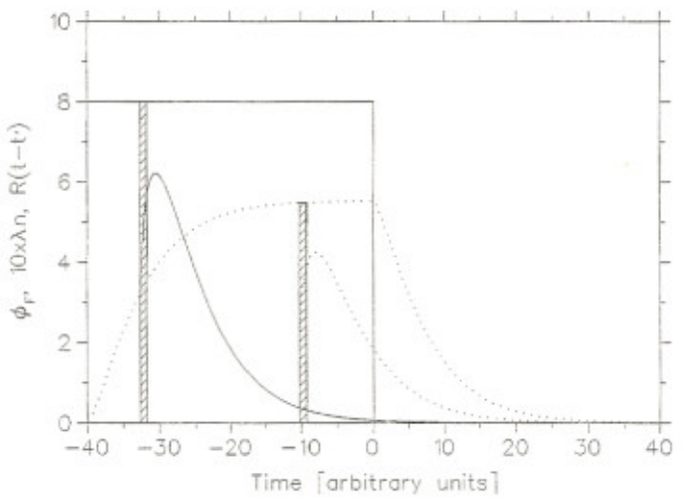

Fig. 1. Principle of calculation of the flux of atoms out of the target. Solid and dashed lines show the fission (ϕ_F) and β decay (λn) contributions, respectively. Each time slice $\mathrm{d}t'$ contributes to the flux at time t via the release function $R(t-t')$. See text for details.

3.2. Finite duration of irradiation

The duration of irradiation is taken into account by integrating Eq. (4) from $-t_{ir}$ up to t_{max} (defined as $t_{max} = t$ if $t<0$ and $t_{max} = 0$ if $t>0$). The flux $\phi(t)$ of atoms is given by following expressions:

$$\phi_F(t<0) = p\sum_k h_k(f_{IRR}(u_k, \bar{t}) - f_{IRR}(v, \bar{t})) \tag{11}$$

$$\phi_F(t>0) = p\sum_k h_k(f_{IRR}(u_k, t_{ir})\,\mathrm{e}^{-u_k t} - f_{IRR}(v, t_{ir})\,\mathrm{e}^{-vt}). \tag{12}$$

The index F stresses that these nuclei are produced directly by fission. For compactness we introduced the notations

$$u_k = \mu_k + \lambda, \quad v = \nu + \lambda, \quad \bar{t} = t + t_{ir}, \quad h_k = \frac{a_k \mu_k \nu}{\nu - \mu_k}$$

and the function

$$f_{IRR}(u,t) = \frac{1-\mathrm{e}^{-ut}}{u}.$$

The flux is a series of exponentials with the same time constants as $R(t)$, but different amplitudes. As it is obvious from Fig. 1, components with short time constants are more strongly attenuated than those with long ones. For long-lasting irradiations leading to a saturation regime one finds back the well-know attenuation factor $\mu_k/(\lambda+\mu_k)$ for each exponential component.

3.3. Decay in target

3.3.1. Introduction to the model

The creation rate is proportional to the number of mother nuclei n_1 in the target. It is difficult to estimate n_1 since it reflects the interplay of the production rate and release time properties. The in-target production rate depends on the own cross-section but also on β decay rate of the parent, i.e. the grand mother of the nucleus of interest. The same argument holds for the number of grand mother nuclei and further up to the most remote precursors, including also those of higher mass due to the phenomenon of β-delayed emission. In the particular case of our measurements with 1 GeV protons cross-sections can be extracted from literature values e.g. Ref. [10]. The sum of cross-sections is an upper limit because a fraction of the precursors may be released before decaying. This fraction is nevertheless small since most release times are long with respect to nuclear halflives of these exotic nuclei. The main approximation is consequently to treat the mother production rate p_1 as if it were due only to the beam, assuming all β feeding mechanisms to occur on a time scale much smaller than the radioactive lifetime of the mother nucleus. We thus use a constant production p_1 rate during irradiation falling to zero when the accelerator beam is switched off.

It is to be noted that the mother atom undergoes its own diffusion and effusion before it decays. Then only part of

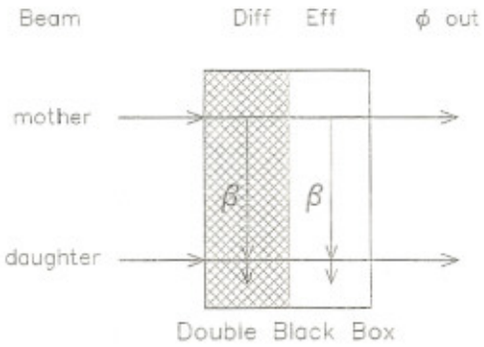

Fig. 2. Schematic model of sequential diffusion and effusion (left to right arrows) including β decay in the target (vertical arrows). See text for details.

the release process of the nucleus of interest remains to be completed. This leads to the schematic model depicted in Fig. 2. The migration of atoms is shown by horizontal arrows from left to right. The nuclei are produced by the interaction of the beam with the matter part of the target represented by the left-hand side box. The time t'' of creation is associated with the left-hand edge of that box. The atoms diffuse, wherefrom the expression 'diffusion box' is used in the following, and then reach the interface of matter and void at time t' (middle vertical line). Then they effuse in the void represented by the right-hand side box (thus 'effusion box') and finally they leave the target at time t (right-hand side edge). In addition, the nucleus of interest is created by β decay either during diffusion or effusion at time t_β (vertical arrows). This extra contribution to the production rate, $p(t_\beta) = \lambda_1 n_1(t_\beta)$, has to be convoluted with the reminder of the release process for the nucleus of interest.

3.3.2. Number of nuclei in target

The first step is therefore to calculate the number of mother nuclei. In either matter (diffusion box) or void (effusion box) they accumulate but are lost by radioactivity and migration. The number of nuclei is given by

$$n(t') = \int_{-t_{ir}}^{t_{max}} p(t'')F_R(t'-t'')\mathrm{e}^{-\lambda(t'-t'')}\,\mathrm{d}t'' \tag{13}$$

where t_{max} is defined as before, F_R is the chance for stable nuclei created at t'' to remain in the target at time t'. It is given by

$$F_R(t) = 1 - \int_0^t R(t')\,\mathrm{d}t' = \int_t^\infty R(t')\,\mathrm{d}t'$$

where $R(t)$ must be replaced with $D(t)$ or $E(t)$ according to the 'box'. The creation rate of nuclei by the beam inside the diffusion box is the beam profile $p(t)$. The number of nuclei is obtained by integration from $-t_{ir}$ up to t_{max} defined as before.

$$n_D(t<0) = p\sum_k a_k f_{IRR}(u_k, \bar{t}) \tag{14}$$

$$n_D(t>0) = p\sum_k a_k f_{IRR}(u_k, t_{ir})\,\mathrm{e}^{-u_k t}. \tag{15}$$

The creation rate of nuclei inside the effusion box is the flux at the interface of the diffusion/effusion boxes. It is obtained from Eq. (4) by setting $D(t)$ for the release function $R(t)$.

$$\phi_{DE}(t<0) = p\sum_k a_k\mu_k f_{IRR}(u_k, \bar{t}) \tag{16}$$

$$\phi_{DE}(t>0) = p\sum_k a_k\mu_k f_{IRR}(u_k, t_{ir})\,\mathrm{e}^{-u_k t}. \tag{17}$$

We note that for each component of the expansion

$$\phi_{DE}(t)_k = \mu_k n_D(t)_k \tag{18}$$

which results from the exponential form adopted for $D_k(t)$. The creation rate in the effusion box $\phi_{DE}(t>0)$ is non-zero after the beam has been switched off. For the calculation of number of nuclei the upper limit of integration is thus now $t_{max} = t$ in both cases. Thus, for $t>0$ there are two terms as a consequence of the different expressions to be inserted for $\phi_{DE}(t)$.

$$n_E(t<0) = p\sum_k a_k\frac{\mu_k}{u_k} f_{ID}(u_k, v, \bar{t}) \tag{19}$$

$$n_E(t>0) = p\sum_k a_k\frac{\mu_k}{u_k}(n_E(a) + n_E(b))$$
$$n_E(a) = f_{ID}(u_k, v, t_{ir})\,\mathrm{e}^{-vt}$$
$$n_E(b) = (1-\mathrm{e}^{-u_k t_{ir}}) f_{DEC}(u_k, v, t). \tag{20}$$

The new functions have been defined

$$f_{DEC}(u, v, t) = \frac{\mathrm{e}^{-ut} - \mathrm{e}^{-vt}}{v-u},$$
$$f_{ID}(u, v, t) = f_{IRR}(v, t) - f_{DEC}(u, v, t).$$

3.3.3. Outgoing flux

In the final step to obtain the flux of nuclei leaving the target the creation rate by β decay is convoluted with the last part of the release process experienced by the nucleus of interest. This leads to

$$\phi_{D\beta}(t) = \int \lambda_1 n_{D1}(t_\beta) R_2(t-t_\beta)\,\mathrm{e}^{-\lambda_2(t-t_\beta)}\,\mathrm{d}t_\beta \tag{21}$$

$$\phi_{E\beta}(t) = \int \lambda_1 n_{E1}(t_\beta) E_2(t-t_\beta)\,\mathrm{e}^{-\lambda_2(t-t_\beta)}\,\mathrm{d}t_\beta. \tag{22}$$

The flux of atoms created via β decay during diffusion is

$$\phi_{D\beta}(t<0) = \lambda_1 p_1 \sum_k \frac{a_{1k}}{u_{1k}} \sum_l h_{2l} \times (f_{ID}(u_{1k}, u_{2l}, \bar{t}) - f_{ID}(u_{1k}, v_2, \bar{t})) \tag{23}$$

and

$$\phi_{D\beta}(t>0) = \lambda_1 p_1 \sum_k \frac{a_{1k}}{u_{1k}} \sum_l h_{2l}(\phi_{Dkl}(a) + \phi_{Dkl}(b))$$

$$\phi_{Dkl}(a) = f_{\mathrm{ID}}(u_{1k}, u_{2l}, t_{\mathrm{ir}})\,\mathrm{e}^{-u_{2l}t} - f_{\mathrm{ID}}(u_{1k}, v_2, t_{\mathrm{ir}})\,\mathrm{e}^{-v_2 t}$$
$$\phi_{Dkl}(b) = (1 - \mathrm{e}^{-u_{1k}t_{\mathrm{ir}}})(f_{\mathrm{DEC}}(u_{1k}, u_{2l}, t) - f_{\mathrm{DEC}}(u_{1k}, v_2, t)). \quad (24)$$

The flux of atoms created via β decay during effusion is

$$\phi_{E\beta}(t<0) = \lambda_1 p_1 \sum_k \frac{a_{1k}\mu_{1k}}{u_{1k}}\, v_2 \phi_{Ek}(a)$$
$$\phi_{Ek}(a) = \frac{f_{\mathrm{ID}}(v_1, v_2, \bar{t})}{v_1} - \frac{f_{\mathrm{DEC}}(u_{1k}, v_2, \bar{t}) - f_{\mathrm{DEC}}(v_1, v_2, \bar{t})}{v_1 - u_{1k}} \quad (25)$$

and

$$\phi_{E\beta}(t>0) = \lambda_1 p_1 \sum_k \frac{a_{1k}\mu_{1k}}{u_{1k}}\, v_2(\phi_{Ek}(a)\mathrm{e}^{-v_2 t} + \phi_{Ek}(b) + \phi_{Ek}(c))$$
$$\phi_{Ek}(a) = \frac{f_{\mathrm{ID}}(v_1, v_2, t_{\mathrm{ir}})}{v_1} - \frac{f_{\mathrm{DEC}}(u_{1k}, v_2, t_{\mathrm{ir}}) - f_{\mathrm{DEC}}(v_1, v_2, t_{\mathrm{ir}})}{v_1 - u_{1k}}$$
$$\phi_{Ek}(b) = f_{\mathrm{ID}}(u_{1k}, v_1, t_{\mathrm{ir}}) f_{\mathrm{DEC}}(v_1, v_2, t)$$
$$\phi_{Ek}(c) = \frac{1 - \mathrm{e}^{-u_{1k}t_{\mathrm{ir}}}}{v_1 - u_{1k}}(f_{\mathrm{DEC}}(u_{1k}, v_2, t) - f_{\mathrm{DEC}}(v_1, v_2, t)). \quad (26)$$

It is logical that when β decay takes place during diffusion the formulae do not contain the effusion constant v_1 of the mother nucleus. Similarly, there are no diffusion constants μ_{2l} of the nucleus of interest when the mother decays during effusion. The final expression for the flux of nuclei of interest is obtained by adding the contribution of the direct production by fission $\phi_{\mathrm{F}}(t)$ and those of β decay, namely $\phi_{D\beta}(t)$ and $\phi_{E\beta}(t)$.

4. Discussion

The formulae contain a too large number of parameters to be of practical use for fitting experimental curves if none of the parameters can be estimated independently. Even if diffusion is described by formulae derived for simple geometries [9], three parameters, μ_0, v and a scale, remain for mother and daughter. Nevertheless, it is interesting to study the limits when either diffusion of effusion times become close to zero, as these can result in different shapes of the release curve. If the diffusion time of the mother nucleus is very fast it does not allow β decay to occur except possibly during effusion. The perturbation of the release curve is then approximated by $\phi_{E\beta}(t)$. Conversely, if the diffusion time is finite but effusion is very quick the perturbation is given by $\phi_{D\beta}(t)$.

In order to carry out reliable release time measurements one should select the experimental conditions to make the contributions of the β delayed functions $\phi_{D\beta}(t)$ and $\phi_{E\beta}(t)$ small compared with the production by fission $\phi_{\mathrm{F}}(t)$. The perturbation is obviously small when the mother nucleus is quickly released, thus giving it little chance to decay in the target. Moreover, as shown by the formula $p(t_\beta) = \lambda_1 n_1(t_\beta)$, the perturbation can be small in two extreme cases of nuclear halflife. A very short lifetime promptly depresses the number of mother nuclei. The nucleus has only a short diffusion path with the properties of the mother element before it decays. Then during most of the remaining time diffusion and effusion properties are those for the nucleus of interest. The time behaviour is the same as the unperturbed one while production rates p_1 and p_2 add up. Alternatively, a mother lifetime considerably longer than the release time of the nucleus of interest reduces the number of decays during the measurement cycles.

An interesting result of the model with two boxes is that an acceleration of the release is also possible. This shall be shown in one of the examples discussed in Section 5.

In the following we indicate some cases where nuclear structure could help to reduce the influence of β decay in target. Large jumps in decay lifetime mostly occur in even-A mass chains. With respect to the average trend the odd–even pairing effects lowers (resp. rises) the masses of even–even (resp. odd–odd) nuclei. This makes the decay energy higher (and the lifetime shorter) if the parent nucleus is odd–odd, and conversely, the lifetime of the even–even daughter is longer.

A long mother halflife can occur close to the valley of β stability where odd-even effects can be larger than the slope of the isobaric mass parabola. Of special importance, because they are easily available by surface ionisation, are the ^{84}Rb and ^{86}Rb isotopes. Their both neighbouring isobars are stable. Moreover, these nuclei have isomers with halflives of 20 and 1.0 min emitting γ rays, thus well suited for the study of release times of short-lived rubidium isotopes. The 3.5 min ^{130}Cs has similar properties. Slightly off stability, even–even nuclei are not stable any longer but still have significantly longer lifetimes than the intermediate odd–odd ones.

Far from stability the decay of a high-spin isomer in an odd–odd nucleus is another way to avoid too much perturbation. Decay of the even–even parent with $I^\pi = 0^+$ hardly reaches such a state. Among Rb and Cs isotopes ^{90}Rb (3^-, 4.3 min) and ^{138}Cs (6^-, 2.9 min) are suitable with respect to halflife and the fact that there exist γ rays almost free of interferences with the decay of the lower-spin ground states.

5. Examples

5.1. Example 1

As first example we compare the release curves of ^{130}Cs^m ($T_{1/2} = 3.46$ min) and ^{139}Cs ($T_{1/2} = 9.27$ min). The isomer in ^{130}Cs is populated only by fission, while ^{139}Cs is also the β daughter of ^{139}Xe ($T_{1/2} = 39.7$ s). The target tested has 'fast' release properties. In this context, the term 'fast' means that the release time constants of cesium are shorter than the Xe parent halflife.

The experimental method is the one described in Section 2. Irradiations have been long enough to reach saturation of the ion currents. We show in Figs. 3 and 4 the part of the release curves after the proton beam has been switched off.

The experimental release curve of ^{130}Cs^m simply corresponds to the flux function $\phi_{\mathrm{F}}(t)$. A fair fit is achieved with

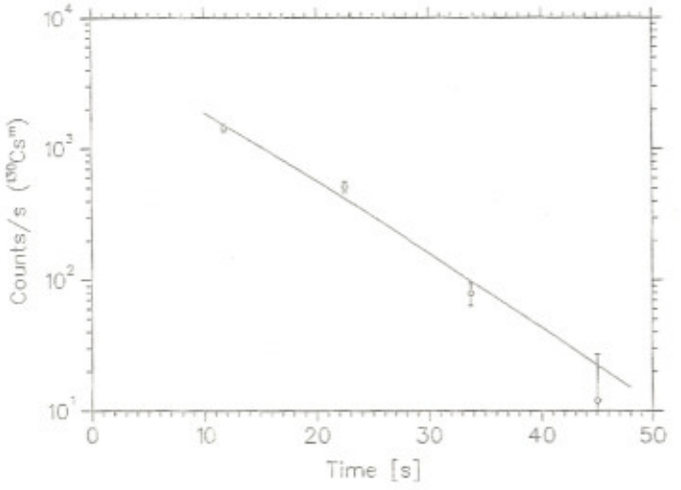

Fig. 3. Release curve for $^{130}Cs^m$. It is fitted with a diffusion component and effusion. see text for details.

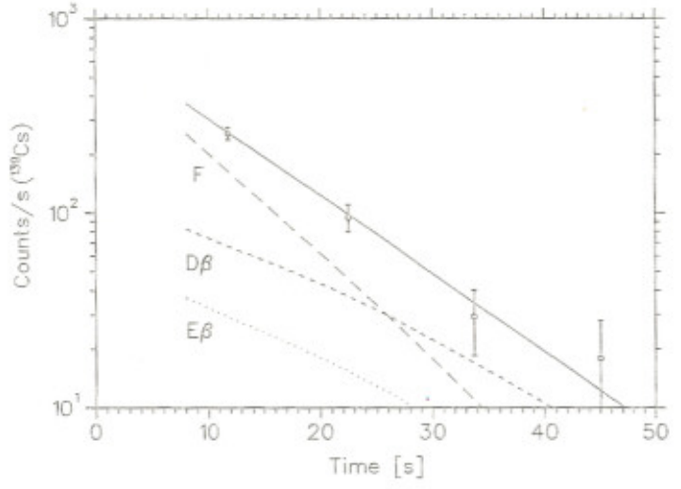

Fig. 4. Release curve for ^{139}Cs. The Cs parameters, except for scaling, are those extracted for $^{130}Cs^m$ and define the function $\phi_F(t)$ (long-dashed line). Xenon parameters are a diffusion and an effusion time resulting in the functions $\phi_{D\beta}(t)$ (short-dashed line) and $\phi_{E\beta}(t)$ (dotted line). The solid line is the sum of the three functions. See text for details.

one exponential which, however, passes above the first point. A better fit is thus possible by considering a sequence of diffusion and effusion. The deduced parameters correspond to $T_\mu(\mathrm{Cs}) = \log(2)/\mu = 5.4(7)\,\mathrm{s}$ and $T_\nu(\mathrm{Cs}) = \log(2)/\nu \simeq 3.0\,\mathrm{s}$, the latter being not well defined.

The β delayed production of ^{139}Cs makes the ion current of ^{139}Cs to fall slower after the accelerator beam is switched off than it does for $^{130}Cs^m$. The release curve of ^{139}Cs is decomposed in the direct production calculated from the ϕ_F function taken from $^{130}Cs^m$, and both contributions of β decay. The relative scales of Xe and Cs in-target productions have been fixed by using experimental cross-sections [10], where for Xe the value used is the sum of $\sigma(\mathrm{Xe})$ and σ's of its β-decay precursors. The Xe release constants are simplified by taking only one diffusion component. The parameters, $T_\mu(\mathrm{Xe}) = 10\,\mathrm{s}$ and $T_\nu(\mathrm{Xe}) = 5\,\mathrm{s}$, are strongly correlated since $\phi_{D\beta}(t)$ and $\phi_{E\beta}(t)$ have a similar shape. Actually, the curves shown in Fig. 4 are not the results of fits with free varying parameters but are calculated. Nevertheless, the scale of the sum of these parameters is important because it controls the amount of Xe decaying in the target. The analysis of the release curve of ^{139}Cs is not very conclusive about the release of Xe, but, at least, it shows that the curve can be reproduced with realistic values.

5.2. Example 2

As another example we analyse release curves of rubidium isotopes for a target with much slower release. We show in Figs. 5 and 6 the decay part of the release curves for $^{86}Rb^m$ ($T_{1/2} = 61\,\mathrm{s}$) and ^{91}Rb ($T_{1/2} = 58\,\mathrm{s}$). Slow release implies that the release parameters (μ_k, ν) are comparable with the radioactive constant λ. They are possibly poorly determined since the fits are sensitive only to the sums $u_k = \lambda + \mu_k$ and $v = \lambda + \nu$. Choosing these Rb isotopes of very similar halflives decreases the impact of possible errors since fits are carried out over the same time range.

The release curve for $^{86}Rb^m$ represents the flux function $\phi_F(t)$. A very good fit is obtained with two exponentials. The parameters ($T_\mu = \log(2)/\mu$, a_k) are (15(3) s, 0.62) and (196 s, 0.38), respectively. The latter is poorly determined due to the short fitting range (50% error). We note that such a good fit is not achieved with a standard diffusion series. The curvature of the curve excludes that one of the constants is associated with effusion (in which case the curve had flattened at the top). Therefore effusion is not observable, i.e. its time constant is much shorter than 15 s.

The release curve of ^{91}Rb exhibits the less usual feature of an extra fast component which has to be associated with

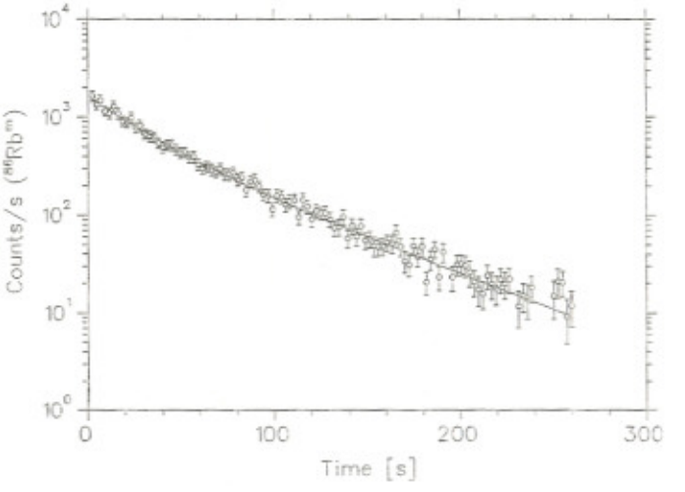

Fig. 5. Release curve for $^{86}Rb^m$. It is empirically fitted with two exponentials associated with diffusion. Since a bend associated with effusion is not seen, effusion is assumed to be much faster than diffusion. See text for details.

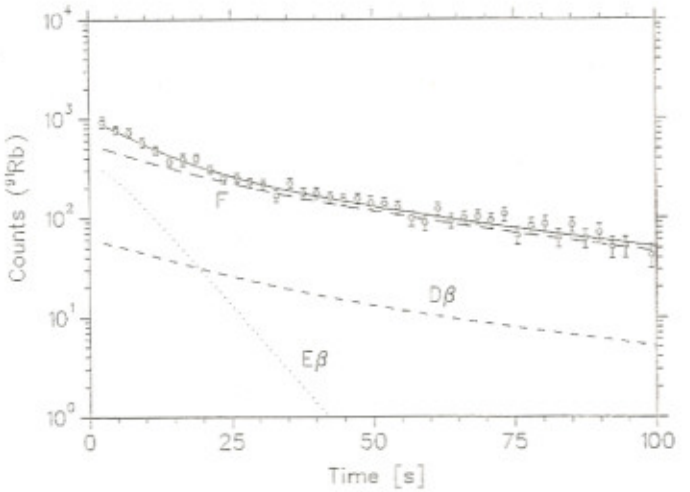

Fig. 6. Release curve for ^{91}Rb. The Rb parameters, except for scaling, are those extracted for ^{86}Rb^{m} and define the function $\phi_F(t)$ (long-dashed line). Krypton parameters are a diffusion and an effusion time resulting in the functions $\phi_{D\beta}(t)$ (short-dashed line) and $\phi_{E\beta}(t)$ (dotted line). The solid line is the sum of the three functions. See text for details.

decay of ^{91}Kr ($T_{1/2} = 8.6$ s). As above, the relative production rates for krypton and rubidium are taken from the measured cross-sections [10]. Beta decay during diffusion (represented by $\phi_{D\beta}(t)$) does not produce a steep enough component at short times. Its time dependence is governed by the slow diffusion of Rb produced after decay. In contrast, the assumed very short effusion time for Rb makes $\phi_{E\beta}(t)$ to be sensitive to Kr parameters and to produce the fast component of the experimental curve. In Fig. 6 the constants used are $T_d(\mathrm{Kr}) = 2$ s and $T_v(\mathrm{Kr}) = 10$ s. These values are not very critical but, nevertheless, a too quick effusion of Kr (i.e. much shorter than the halflife of ^{91}Kr) would suppress the probability of the enhanced release exhibited by $\phi_{E\beta}(t)$.

6. Conclusion

We have developed a framework for the empirical analysis of release curves of radioactive nuclei. It allows to implement the production of the nucleus of interest via β decay in the target, which is able to significantly modify the release curves. The perturbation is small in case the extra feeding $\lambda n(t)$ is small against the direct production rate. This could happen, e.g. when the mother nucleus is quickly removed from the target by its fast own release (making $n(t)$ small) or has little chance to decay ($\lambda < \mu_k$, v of the nucleus of interest). The model is flexible, as it has been shown with examples, but its drawback is a large number of parameters. These are too many to be extracted from a single release curve. If it is not possible to find cases where nuclear properties prevent feeding by β decay, the model gives hints to find those with small perturbation. If this is neither possible the parameters can be constrained by analysing curves recorded for various mass chains, since release depends on the element and not on its isotope.

Acknowledgements

The authors are indebted to Drs. D.V. Fedorov, A.M. Ionan, V.S. Ivanov, S.Yu. Orlov, A.G. Polyakov and Yu.M. Volkov for running the on-line mass separator at the IRIS facility at Gatchina, and further to Drs. P. Jardin and B. Roussière, for stimulating discussions about the mechanism of diffusion and about measurement method at PARRNe.

We acknowledge the financial support of the European Community under the FP6 "Research Infrastructure Action—Structuring the European Research Area" EURISOL DS Project Contract No. 515768 RIDS. The EC is not liable for any use that may be made of the information contained herein.

References

[1] R. Kirchner, Nucl. Instr. and Meth. B 204 (2003) 179 and refs. therein.
[2] A. Bracco, A. Pisent, LNL-INFN (REP) 181/02 (2002).
[3] (http://www.ganil.fr/research/developments/spiral2/index.html).
[4] (http://www.lnl.infn.it/~eurisol/index.php).
[5] A. Andrighetto, et al., Nucl. Instr. and Meth. 204 (2003) 267.
[6] A. Andrighetto, et al., Eur. Phys. J. A 19 (2004) 341.
[7] A. Andrighetto, et al., Eur. Phys. J. A 23 (2005) 257.
[8] B. Roussière, et al., Nucl. Instr. and Meth. B 194 (2002) 151.
[9] R. Kirchner, Nucl. Instr. and Meth. B 70 (1992) 186.
[10] M. Bernas, et al., Nucl. Phys. A 725 (2003) 213.